

Supporting Information

Ultrasmall Renally-clearable Silica Nanoparticles Target Prostate Cancer

Feng Chen,^{[a],†} Kai Ma,^{[b],†} Li Zhang,^[a] Brian Madajewski,^[a] Melik Z. Turker,^[b] Fabio Gallazzi,^[c] Kiara Cruickshank,^[a] Xiuli Zhang,^[d] Pocharapong Jenjiranant,^[a] Karim A Touijer,^[e] Thomas P. Quinn,^[d,f] Pat Zanzonico,^[g] Ulrich Wiesner,^{*[b]} Michelle S. Bradbury^{*[a,h]}

^[a]Department of Radiology, Sloan Kettering Institute for Cancer Research, New York, NY 10065, USA;

^[b]Department of Materials Science & Engineering, Cornell University, Ithaca, NY 14853, USA

^[c]Department of Chemistry and Molecular Interactions Core, University of Missouri, Columbia, MO 65211, USA

^[d]Department of Biochemistry, University of Missouri, Columbia, MO 65211, USA;

^[e]Urology Service, Department of Surgery, Memorial Sloan Kettering Cancer Center, New York, NY, 10065, USA

^[f]Harry S Truman Veterans' Hospital, Columbia, MO 65201 USA

^[g]Department of Medical Physics, Memorial Sloan Kettering Cancer Center, New York, NY 10065, USA

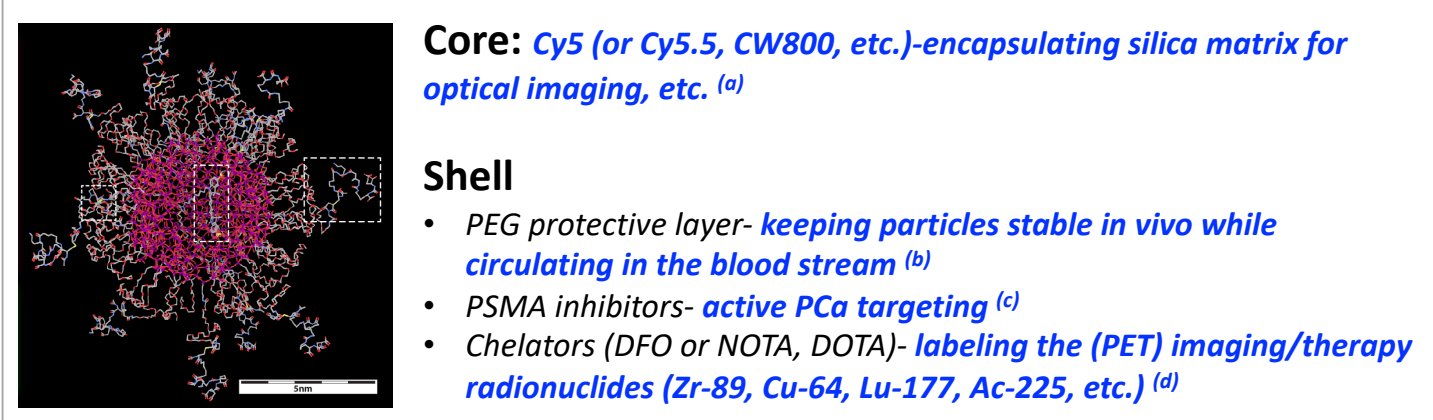
^[h]Molecular Pharmacology Program, Sloan Kettering Institute for Cancer Research, New York, NY 10065, USA

† Dr. F. Chen and Dr. K. Ma contributed equally to this work

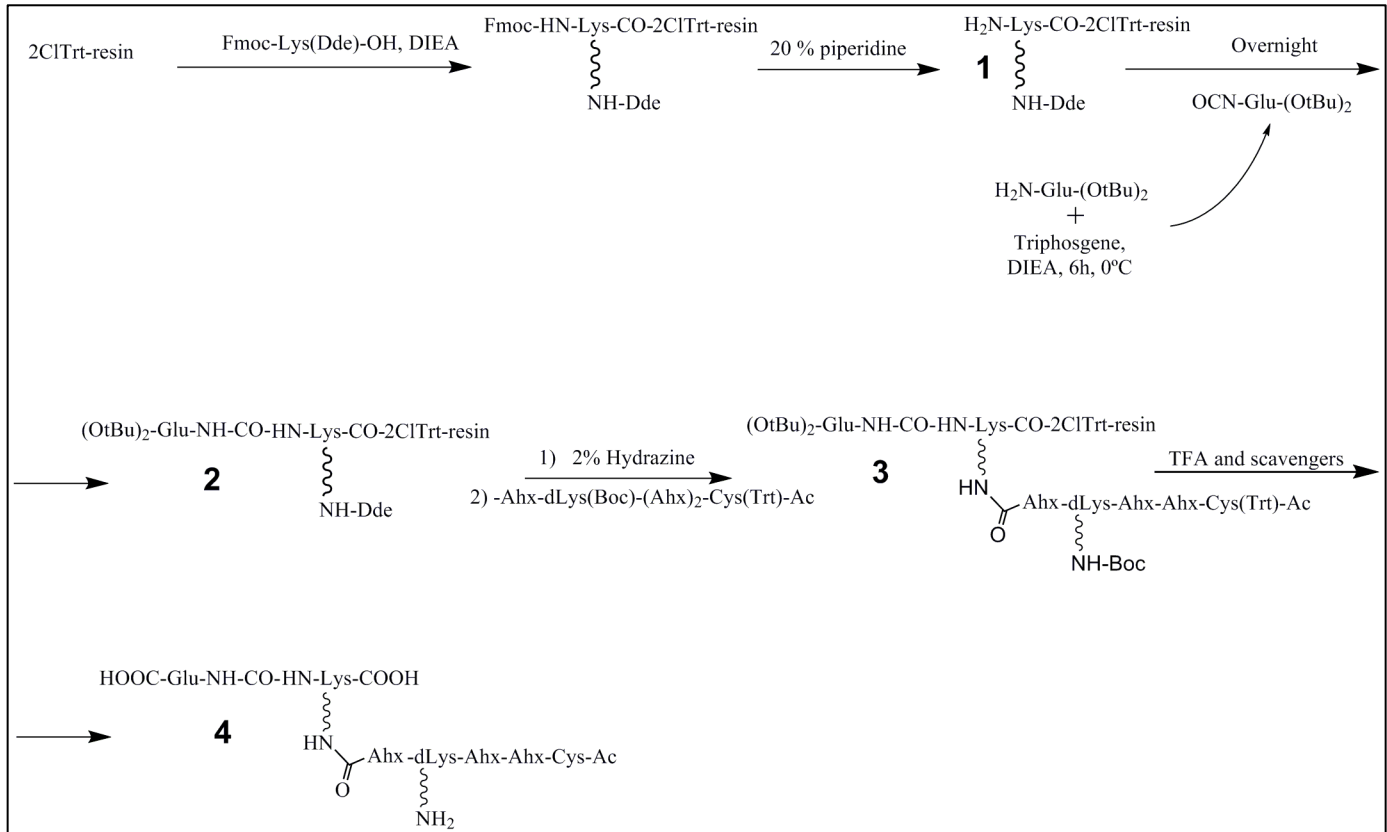
*Correspondence and requests for materials should be addressed to: M. S. Bradbury (bradburm@mskcc.org) and U. Wiesner (ubw1@cornell.edu)

Supplementary Figures and Tables

Scheme S1. A schematic illustration showing the core-shell structure of the ultrasmall silica-based PSMA-targeting PET/optical dual-modality nanoparticles, *i.e.*, ^{89}Zr -DFO-PSMAi-PEG-Cy5-C' dots. **(a)** We designed the **core** to consist of a silica matrix that covalently encapsulates organic dyes like Cy5 (or Cy5.5, CW800, etc.) for (1) obtaining key particle parameters of particle size (nm) and concentration (nM) by using fluorescence correlation spectroscopy (FCS), and concomitantly (2) to facilitate the applications of *in vitro* cell binding using flow cytometry, *in vivo* small animal optical imaging using the IVIS® Spectrum *in vivo* imaging system, *ex vivo* tissue analysis, and intraoperative large animal/human image-guided surgery using FDA-cleared Quest Spectrum® fluorescence imaging system. The physical size of the core is carefully controlled to a diameter of 3-4 nm using a water-based C' dot synthesis technique.¹ We then cover the core with a functional **shell** which includes **(b)** a dense polyethylene glycol (MW: ~500 g/mol) brush layer for stabilizing the ultrasmall silica core against aggregation in water (or phosphate-buffered saline [PBS], cell culture media, *etc.*) and in the bloodstream; **(c)** prostate-specific membrane antigen inhibitor (PSMAi) for active PCa targeting. The PSMAi was first conjugated to PEG-silane and then reacted with the core surface *via* hydrolysis and condensation; **(d)** radionuclide chelators of deferoxamine (DFO) (or 1,4,7-Triazacyclononane-1,4,7-triacetic acid [NOTA], 1,4,7,10-Tetraazacyclododecane-1,4,7,10-tetraacetic acid [DOTA]) for labeling with positron emitting radionuclides of ^{89}Zr (or ^{64}Cu), or therapeutic radionuclides of ^{177}Lu (or ^{225}Ac).



Scheme S2. A schematic illustration of the synthesis of PSMAi peptide.



Scheme S3. A schematic illustration of the synthesis of PSMAi-PEG-silane and Cy5-silane.

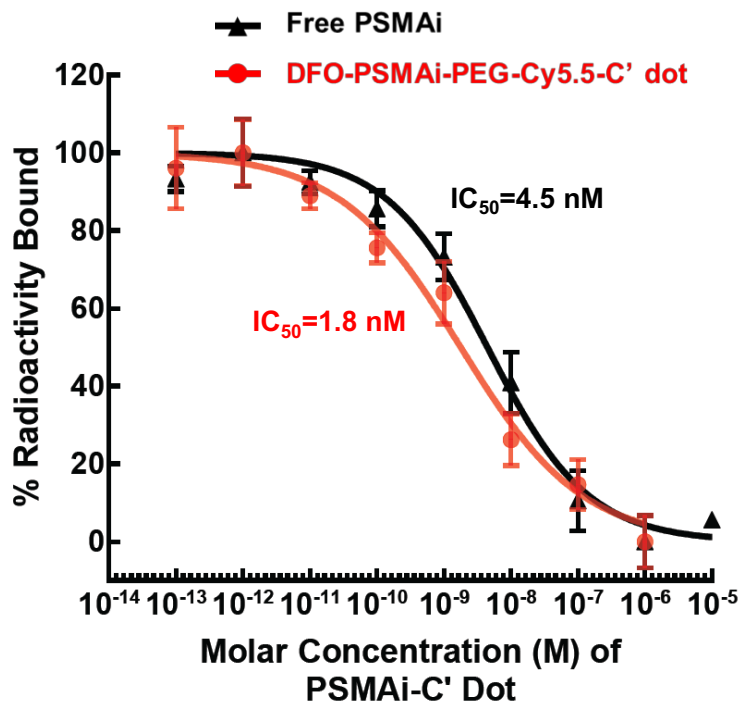
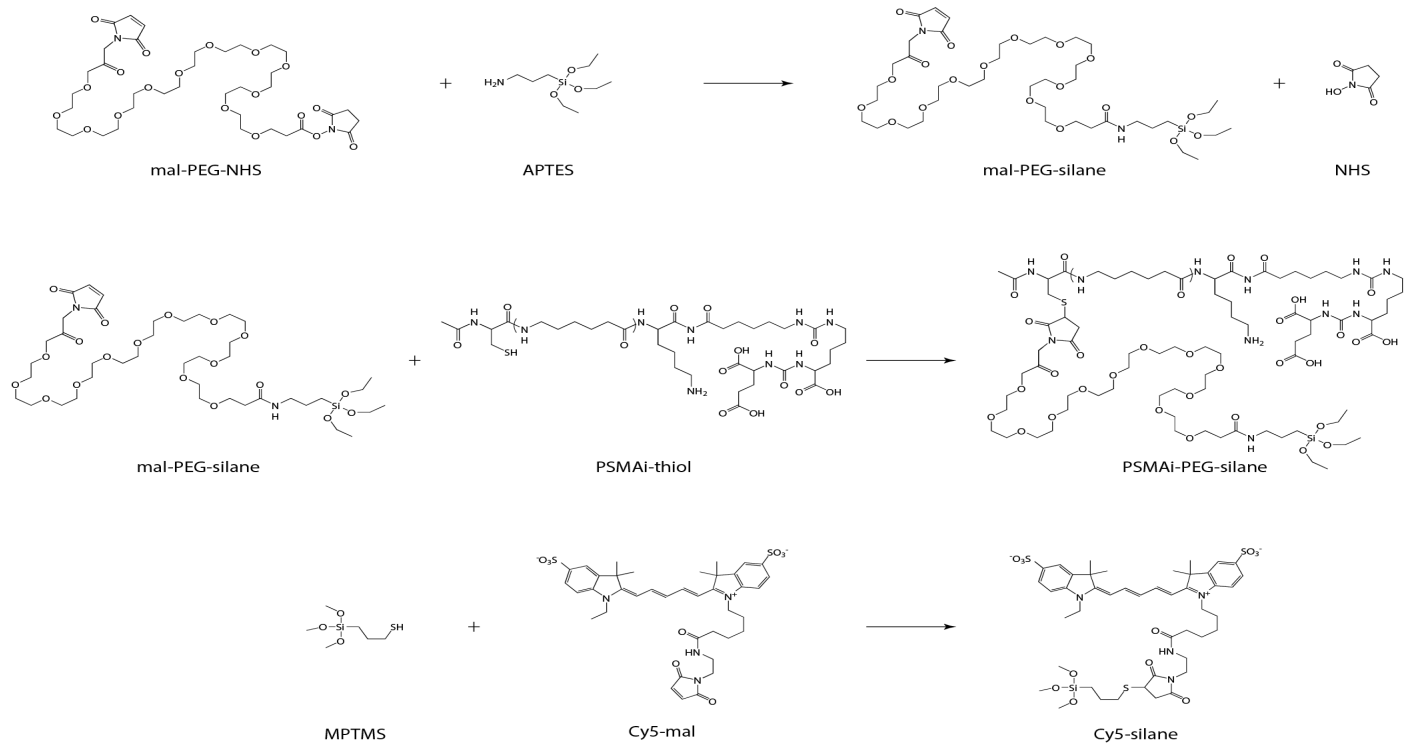


Figure S1. IC₅₀ comparison between free PSMAi peptides and DFO-PSMAi-PEG-Cy5.5-C' dots.

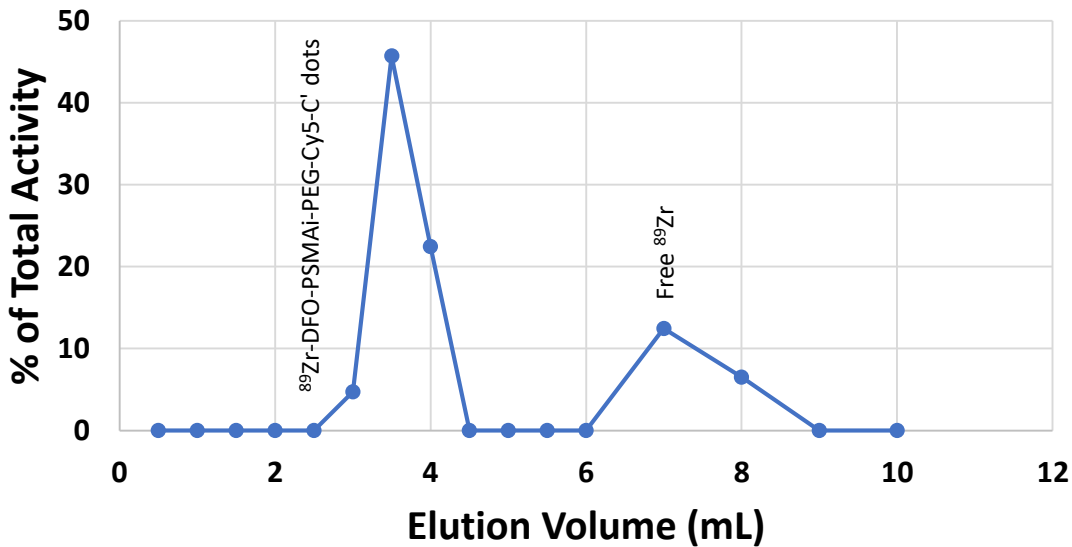


Figure S2. Representative PD-10 elution profile of ^{89}Zr -DFO-PSMAi-PEG-Cy5-C' dots. ^{89}Zr labeling yield was found to be 70-80% ($n>5$) with a specific activity of >1000 Ci/mmol. The ^{89}Zr -DFO-PSMAi-PEG-Cy5-C' dot product eluted between 2.5 mL and 4.0 mL, while the free ^{89}Zr eluted between 6 mL and 9 mL.

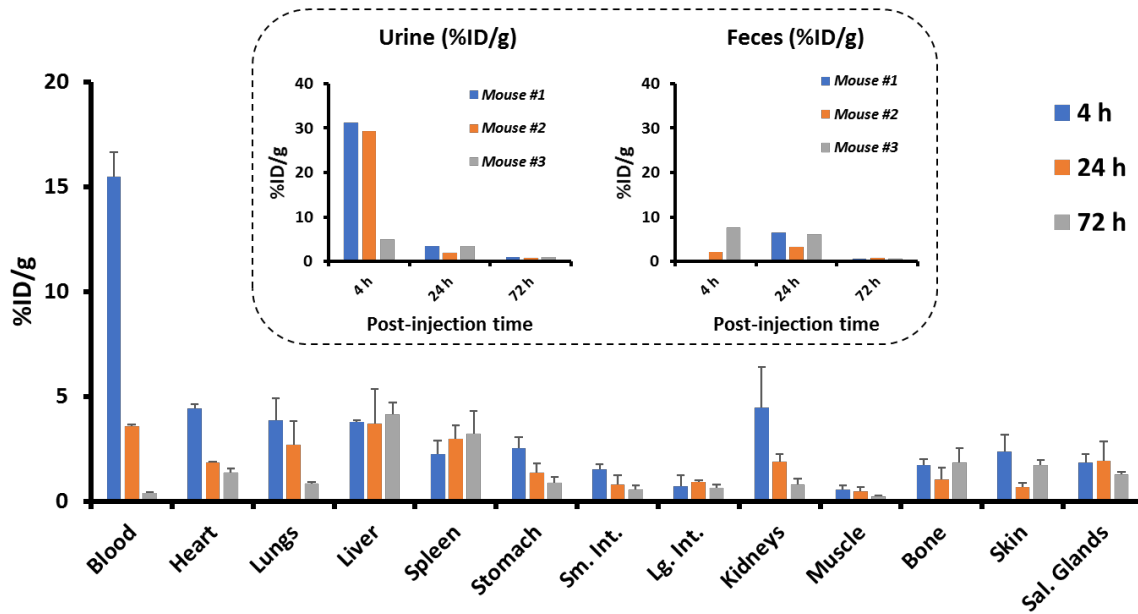


Figure S3. Biodistribution of ^{89}Zr -DFO-PSMAi-PEG-Cy5-C' dots in major organs and tissues of normal, healthy mice (presented as %ID/g) at 4, 24 and 72 h post-injection ($n=3$). **Please note**, all mice were kept in regular cages. Urine samples were collected directly from mouse bladders during the study. The %ID/g number of urine varied significantly from mouse to mouse at early post-injection time points. For more accurate measurement of the renal (or hepatic) clearance of ^{89}Zr -DFO-PSMAi-PEG-Cy5-C' dots, we also performed a metabolic cage study (**Fig. 2B**) where all urine and fecal specimens were separately collected.

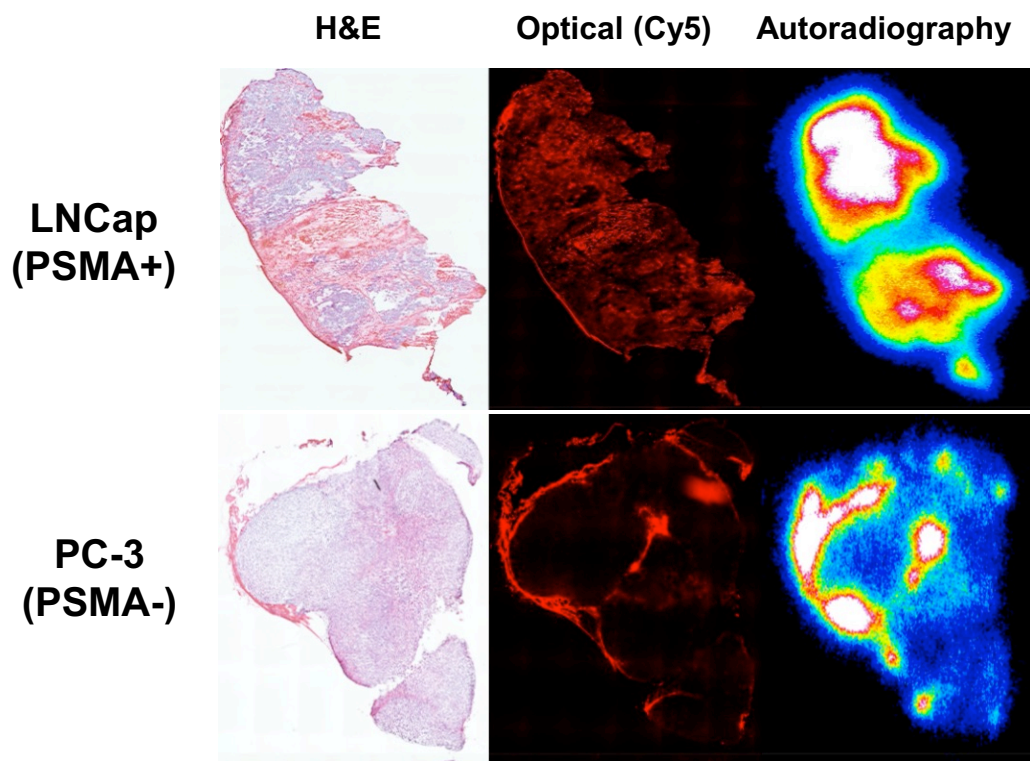


Figure S4. Correlative *ex vivo* tumor histopathology. From left to right: (Left) H&E stained tumor tissue specimens harvested at 72 h post-injection; (Middle) Cy5-fluorescence microscopy images; (Right) autoradiography images of the same tumor specimens.

Table S1. The cumulative clearance of ^{89}Zr -DFO-PSMAi-PEG-Cy5-C' dots in mouse urine and feces at different post-injection time points (n=3). Note, the radioactivity in both urine and feces was measured using a CRC®-55tR Dose Calibrator and presented as %ID (mean \pm SD).

<i>Post-injection time pints</i>	<i>Urine</i>		<i>Feces</i>		<i>Urine/Feces Ratio</i>	
	<u>(%ID, n=3)</u>		<u>(%ID, n=3)</u>			
	<i>Ave.</i>	<i>Std.</i>	<i>Ave.</i>	<i>Std.</i>		
4 h	26.4	3.6	0.01	0.01	5102.0	
24 h	41.0	4.0	11.6	2.5	3.5	
48 h	46.0	4.1	17.8	1.6	2.7	
72 h	49.1	4.3	19.0	1.3	2.6	
144 h	51.7	4.1	20.2	1.7	2.6	
168 h	52.6	4.0	20.3	1.7	2.6	

Table S2. *Ex vivo* biodistribution data of ^{89}Zr -DFO-PSMAi-PEG-C' dots at 168 h (on Day 7) post-injection (n=3, from the metabolic cage study). Radioactivity in major organs and tissues was measured using a gamma-counter and presented as **%ID** (mean \pm SD).

168 h p.i. (%ID)	^{89}Zr -DFO-PSMAi-PEG-C' dots (%ID, n=3)	
	<i>Ave.</i>	<i>Std.</i>
Blood	0.1	0.0
Heart	0.1	0.0
Lungs	0.1	0.0
<u>Liver</u>	<u>1.3</u>	0.2
Spleen	0.1	0.1
Stomach	0.1	0.0
Sm. Int.	0.2	0.0
Lg. Int.	0.1	0.0
<u>Kidneys</u>	<u>0.2</u>	0.1
Brain	0.0	0.0
<u>Salivary Gland</u>	<u>0.2</u>	0.0
<u>Carcass</u>	<u>16.3</u>	1.7
<u>Feces</u>	<u>20.3</u>	1.7
<u>Urine</u>	<u>52.6</u>	4.0

Table S3. *Ex vivo* biodistribution data of ^{89}Zr -DFO-PSMAi-PEG-Cy5-C' dots at 4, 24 h and 72 h post-injection (n=3). Radioactivity in major organs and tissues was measured using a gamma-counter and presented as **%ID/g** (mean \pm SD).

%ID/g	4 h		24 h		72 h	
	Ave.	Std.	Ave.	Std.	Ave.	Std.
Blood	15.5	1.1	3.6	0.1	0.4	0.0
Heart	4.4	0.2	1.9	0.0	1.4	0.2
Lungs	3.9	1.0	2.7	1.1	0.8	0.1
Liver	3.8	0.1	3.7	1.7	4.2	0.6
Spleen	2.3	0.6	3.0	0.7	3.2	1.1
Stomach	2.5	0.5	1.4	0.4	0.9	0.3
Sm. Int.	1.5	0.2	0.8	0.4	0.6	0.2
Lg. Int.	0.7	0.5	0.9	0.1	0.6	0.2
Kidneys	4.5	1.9	1.9	0.4	0.8	0.3
Muscle	0.5	0.2	0.5	0.2	0.2	0.1
Bone	1.7	0.3	1.0	0.6	1.8	0.7
Skin	2.4	0.8	0.7	0.2	1.7	0.3
Salivary Glands	1.8	0.4	1.9	0.9	1.3	0.1

Table S4. Radiation dosimetry of ^{89}Zr -DFO-PSMAi-PEG-Cy5-C' dots in a 70-kg standard man estimated by using the OLINDA dosimetry program. For comparison, absorbed doses are also shown for the ^{89}Zr -labeled PSMA-targeted minibody (i.e., ^{89}Zr -IAb2M)² and antibody (i.e., ^{89}Zr -huJ591)³.

	Absorbed Dose (mGy/mBq)		^{89}Zr -huJ591 (antibody, 150 kDa) (c)	Comparison	
	^{89}Zr -DFO-PSMAi-PEG-Cy5-C' dots (nanoparticle, ~110 kDa)	^{89}Zr -IAb2M (minibody, 80 kDa) ^(b)		Absorbed dose ratio (minibody vs C' dot)	Absorbed dose ratio (antibody vs C' dot)
Adrenals	0.102	0.53	0.55	5.2	5.4
Brain	0.052	0.17	0.14	3.3	2.7
Gallbladder Wall	0.121	0.73	0.75	6.0	6.2
Lower Large Intestine Wall	0.094	0.49	0.22	5.2	2.3
Small Intestine	0.098	0.36	0.29	3.7	3.0
Stomach Wall	0.071	0.35	0.33	4.9	4.7
Upper Large Intestine Wall	0.096	0.45	0.33	4.7	3.4
Heart Wall	0.101	0.69	0.86	6.8	8.5
Kidneys	0.082	1.36	0.95	16.7	11.6
Liver	0.276	1.67	2.08	6.1	7.5
Lungs	0.104	0.52	0.58	5.0	5.6
Muscle	0.067	0.25	0.23	3.7	3.4
Pancreas	0.096	0.5	0.5	5.2	5.2
Red Marrow	0.130	0.32	0.32	2.5	2.5
Skin	0.042	0.17	0.16	4.0	3.8
Spleen	0.179	0.76	0.74	4.2	4.1
Testes	0.049	0.19	0.16	3.9	3.3
Thymus	0.061	0.31	0.31	5.1	5.1
Thyroid	0.056	0.21	0.19	3.8	3.4
Urinary Bladder Wall	0.134	0.25	0.21	1.9	1.6
Salivary Glands	0.041	NA	NA	NA	NA
Total Body	0.079	0.3	0.29	3.8	3.7

(a) 1 Gy (or J/kg) of Gamma absorbed dose corresponds to 1 Sv of equivalent dose

(b) The minibody IAb2M is genetically engineered from huJ591

(c) The humanized antibody J591 (huJ591) directly targets the extracellular domain of the PSMA

References

- (1) Ma, K.; Mendoza, C.; Hanson, M.; Werner-Zwanziger, U.; Zwanziger, J.; Wiesner, U. Control of Ultrasmall Sub-10 nm Ligand-Functionalized Fluorescent Core–Shell Silica Nanoparticle Growth in Water. *Chem Mater* **2015**, *27*, 4119–4133.
- (2) Pandit-Taskar, N.; O'Donoghue, J. A.; Ruan, S.; Lyashchenko, S. K.; Carrasquillo, J. A.; Heller, G.; Martinez, D. F.; Cheal, S. M.; Lewis, J. S.; Fleisher, M.; Keppler, J. S.; Reiter, R. E.; Wu, A. M.; Weber, W. A.; Scher, H. I.; Larson, S. M.; Morris, M. J. First-in-Human Imaging with ^{89}Zr -Df-IAB2M Anti-PSMA Minibody in Patients with Metastatic Prostate Cancer: Pharmacokinetics, Biodistribution, Dosimetry, and Lesion Uptake. *J Nucl Med* **2016**, *57*, 1858–1864.
- (3) Pandit-Taskar, N.; O'Donoghue, J. A.; Beylergil, V.; Lyashchenko, S.; Ruan, S.; Solomon, S. B.; Durack, J. C.; Carrasquillo, J. A.; Lefkowitz, R. A.; Gonen, M.; Lewis, J. S.; Holland, J. P.; Cheal, S. M.; Reuter, V. E.; Osborne, J. R.; Loda, M. F.; Smith-Jones, P. M.; Weber, W. A.; Bander, N. H.; Scher, H. I.; Morris, M. J.; Larson, S. M. ^{89}Zr -huJ591 immuno-PET imaging in patients with advanced metastatic prostate cancer. *Eur J Nucl Med Mol Imaging* **2014**, *41*, 2093–2105.